All-channel tunable optical dispersion compensator based on linear translation of a waveguide grating router

David Sinefeld,[1,*] Shalva Ben-Ezra,[2] Christopher R. Doerr,[3] and Dan M. Marom[1]

[1]*Applied Physics Department, Hebrew University, Jerusalem 91904, Israel*

[2]*Finisar Corporation, Nes Ziona, Israel*

[3]*Bell Laboratories, Alcatel-Lucent, 791 Holmdel-Keyport Road, Holmdel, New Jersey 07733, USA*

**Corresponding author: sinefeld@gmail.com*

Received January 7, 2011; revised February 28, 2011; accepted March 14, 2011; posted March 17, 2011 (Doc. ID 140761); published April 13, 2011

We propose and demonstrate a compact tunable optical dispersion compensation (TODC) device with a 100 GHz free spectral range capable of mitigating chromatic dispersion impairments. The TODC is based on longitudinal movement of a waveguide grating router, resulting in chromatic dispersion compensation of ± 1000 ps/nm. We employed our TODC device for compensating 42.8 Gbit/sec differential phase-shifting keying signal, transmitted over 50 km fiber with a -2 dB power penalty at 10^{-9}. © 2011 Optical Society of America

OCIS codes: 060.2330, 130.2035.

Tunable optical dispersion compensation (TODC) devices are essential components in direct detection, high bit rate communication channels, as broad signal spectrum and narrow bit periods result in sensitivity to dispersion-induced intersymbol interference. Oftentimes, the TODC device needs to be colorless, having a free spectral range (FSR) matching the channel spacing, enabling multichannel compensation in wavelength division multiplexed (WDM) networks and reducing inventory. Colorless TODC devices can be based on ring resonators [1], sampled chirped fiber Bragg gratings [2], and Mach–Zehnder interferometers [3]. A special category of TODC devices is based on the combination of a dispersion element and a spatially controlled phase. The channel-matched FSR dispersion element can be an etalon [4], virtually imaged phased array [5], or waveguide grating router (WGR) [6], whereas the phase element may be a mirror with various selectable curvatures [7], a deformable mirror [8], a rotating cylindrical lens [9], a polymer thermo-optic lens [10], or a phase spatial light modulator (SLM) [11–13]. Common to these elements is the requirement of applying a quadratic phase function across the dispersed signal in an adjustable fashion.

Here we present a compact TODC device based on an extremely simple free space arrangement of a WGR, Fourier lens, and flat reflecting mirror [14,15], with accompanying 42.8 Gb/sec transmission results. Whereas other TODC utilized spatially controlled quadratic phase elements at the Fourier plane [7–13] or a relatively simple movement with a complex optical setup [5] impacting TODC device complexity and cost, we use a very compact arrangement and simply modify the distance between the WGR and the Fourier lens. The longitudinal displacement is equivalent to applying a radial phase at the Fourier plane and results in a curved phase front added to the dispersed spectral components. In this way we can compensate for chromatic dispersion (CD) values up to ± 1000 ps/nm. Since our WGR has a free spectral range of 100 GHz, the phase curvature is applied simultaneously to all WDM channels on the channel plan, resulting in colorless device operation. The simplicity of this system makes it effective as a TODC device for mitigating dispersion impairments, as it consumes no power once set and hence will not fail in power outages. The longitudinal displacement of the WGR from the front focal plane (distance f to lens) to an arbitrary distance d (between WGR and lens) results in a quadratic phase added to the beam at Fourier plane with curvature [16]:

$$\frac{1}{R}=\frac{1}{f}\left(1-\frac{d}{f}\right). \tag{1}$$

As was shown in previous works [11,12,15], this curvature results in applied CD values according to

$$\mathrm{CD}=\frac{2\lambda_0}{c_0}\frac{1}{R}\left(\frac{dx}{d\lambda}\right)^2=\frac{2\lambda_0}{c_0}\left(\frac{dx}{d\lambda}\right)^2\frac{\Delta z}{f^2}=\frac{2\lambda_0}{c_0}\left(\frac{d\theta}{d\lambda}\right)^2\Delta z, \tag{2}$$

where $\Delta z=f-d$. Hence, CD values have a linear dependence on the displacement Δz between the WGR and the Fourier lens. In this way, very simple longitudinal translation of the WGR results in different CD compensation values.

The TODC device layout and concept is depicted in Fig. 1. Light enters through an input/output waveguide to a planar lightwave circuit (PLC) containing an extremely high-resolution silica-on-silicon WGR with 0.8% index contrast waveguides that consists of 34 grating arms that are "pinched" in the middle for conserving wafer area, reducing the grating sensitivity to wafer refractive index and fabrication gradients, and enables the insertion of a half-wave plate to make the WGR polarization independent (not implemented in the present system). The angular dispersion $d\theta/d\lambda$ at the output facet of the PLC is converted to spatial dispersion with a $f=50$ mm Fourier lens, resulting in a spatial dispersion along the x axis. A $f=3$ mm cylindrical lens collimates the radiated light from the WGR in the guided (slab) direction to reduce the output numerical aperture. A circulator was used to separate the input and output light to the PLC. The insertion loss of the TODC device is -12.5 dB. This high loss value is partially due to phase errors in the fabricated WGR, as well as an unoptimized transition from the guided region to free space. Both issues can be corrected in a subsequent run. We anticipate system losses of ~5 dB can be achieved, limited by WGR coupling inefficiency.

0146-9592/11/081410-03$15.00/0

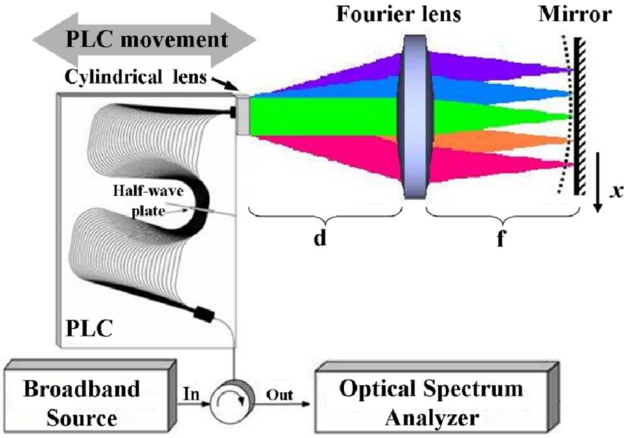

Fig. 1. (Color online) Layout of the tunable optical dispersion compensator. Changing the distance d between the WGR and the Fourier lens imparts a quadratic phase across the Fourier plane (seen as a dashed surface on the Fourier plane).

In order to determine the dispersion along the x axis ($dx/d\lambda$ value), we placed a needle in the Fourier plane and moved it along the x axis, finding for each position the corresponding attenuated wavelength component. In this way we have found that $dx/d\lambda = 5.4\,\mathrm{mm/nm}$. We repeated this measurement for both TE and TM polarizations and obtained similar results (5.4 and 5.3 mm/nm). Since the free space arrangement does not depend on polarization, the source of the slight polarization dependence is the WGR birefringence. The effect of birefringence is a polarization-dependent splitting of the spectral passband; however, both polarizations would incur the same dispersion setting.

As a first test of the TODC device, we changed the distance d between the WGR and the Fourier lens along

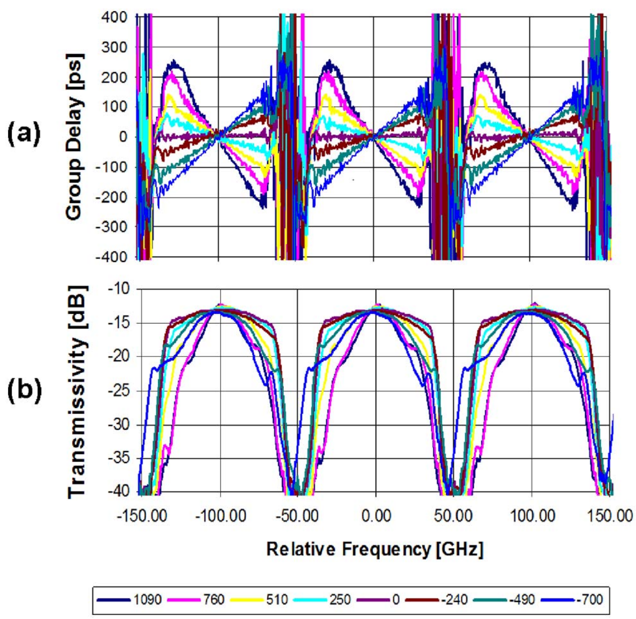

Fig. 2. (Color online) CD compensation results. (a) Group delay versus frequency. Linear slopes are observed, corresponding to eight different dispersion values between −700 and 1100 ps/nm. (b) Transmissivity versus frequency. Spectral narrowing is observed for increasing departures from zero dispersion. Passband and dispersion settings are repeated at 100 GHz FSR.

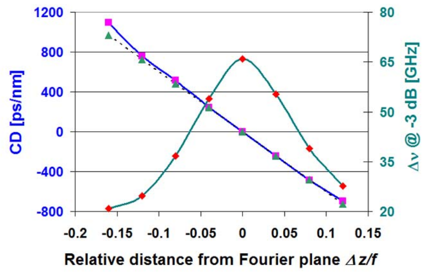

Fig. 3. (Color online) Measured CD values (blue), theoretical CD values (black dashed curve), and bandwidth (green with a peak) versus displacement Δz. As the phase curvature values at the Fourier plane are larger, the narrowing effect becomes dominant: bandwidth is reduced down to 20 GHz for CD values of ± 1000 ps/nm.

14 mm travel and measured the group delay (GD) and the transmissivity at several positions. The GD varied linearly within the TODC FSR, a testament of TODC action (Fig. 2). As one can expect from such a system, the quadratic phase imposes not only CD but also an undesired spectral narrowing, due to the tilt applied to spectral components far from the channel grid. The measured CD values (calculated from the GD slopes), the theoretical CD values (using Eq. (2), with the experimental $dx/d\lambda$ values), and the resulting −3 dB channel bandwidth measures are plotted in Fig. 3 against the relative displacement from the lens front focal plane $\Delta z/f$. The experimental and theoretical CD values match extremely well. As the phase curvature values at the Fourier plane increase, the narrowing effect becomes dominant, and the bandwidth is reduced down from 65 GHz at low CD correction values to 20 GHz for extreme TODC values of ± 1000 ps/nm. In principle, there is an option of eliminating the bandwidth narrowing by using a four pass system [13,17]; however, such a system is more complicated and will suffer higher losses.

Polarization-dependent loss (PDL) and polarization-mode dispersion (PMD) were measured (Fig. 4), to examine the effect of PLC birefringence. The results reveal that within the central 65 GHz, the PDL is lower than 0.3 dB and the PMD is less than 5 ps. These effects are

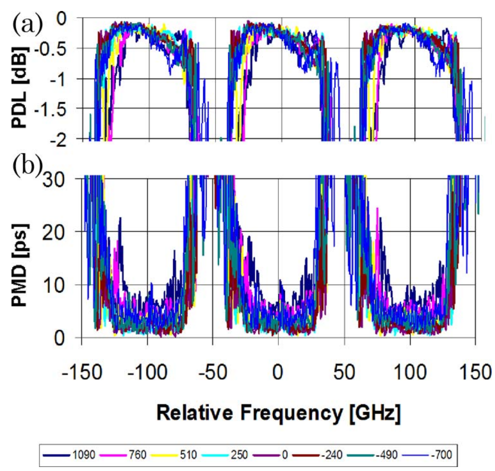

Fig. 4. (Color online) (a) Polarization-dependent loss (PDL) measured in dB versus relative frequency, (b) polarization-mode dispersion (PMD) measured in ps versus relative frequency.

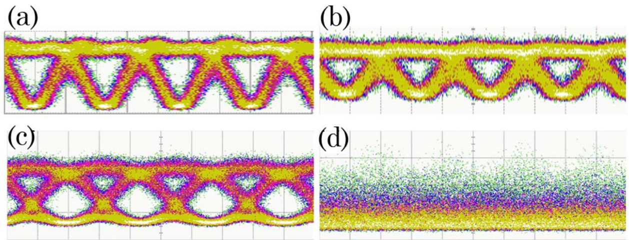

Fig. 5. (Color online) Detected eye diagrams after TODC correction with signal transmitted along (a) 0 km, (b) 20 km, (c) 40 km, and (d) 40 km without TODC CD correction.

caused solely by the birefringence of the PLC, since all the free space optics elements are polarization insensitive. Insertion of the optional half-wave plate at the pinched point of the WGR should eliminate this entirely.

The dispersion compensation capability of the TODC device was tested using a 42.8 Gb/s differential phase-shift keying $2^{31}-1$ pseudorandom bit sequence at 1550.12 nm, with different lengths of standard single-mode fiber (dispersion coefficient of 17 ps/nm-km) placed between the transmitter and the receiver. Tuning the TODC device was trivial, as a single micrometer movement yielded immediate eye opening at the proper distance Δz, as shown in Fig. 5. Without the dispersing fiber, the TODC showed zero penalty over the back-to back case, as can be seen in Fig. 6. The penalty for compensation of 30–50 km fiber length was ~2 dB optical signal-to-noise ratio (OSNR)at 10^{-9} bit error ratio (BER). For the 60 km fiber length, the penalty increased. We attribute the greater penalty to passband narrowing at our chosen modulation format. This bandwidth narrowing changes the signal quality, as seen in the eye shape [Fig. 5(c)], resembling that of doubinary modulation [18,19].

In this work we have shown a very simple, compact apparatus for TODC. In fact, actual systems that will be based on this scheme could become even more compact by use of a Fourier lens with very short focal length. Since the beam size at the output of the PLC is approximately 0.5 mm, a few millimeter focal length lens could be substituted over our 50 mm lens, resulting in a compact TODC arrangement. The PLC travel range of such a system will also be reduced, resulting in a compact system with a relatively large dispersion tuning range. Another advantage of this kind of system is that in the case of failure the tuning condition remains fixed. Note that the TODC might require temperature stabilization for holding the WDM grid position, an issue that was not examined in this work. However, this stabilization is identical to all WGR-based devices (e.g., a demultiplexer), as the shift does not depend on the diffraction order of the WGR (i.e., no increased temperature sensitivity).

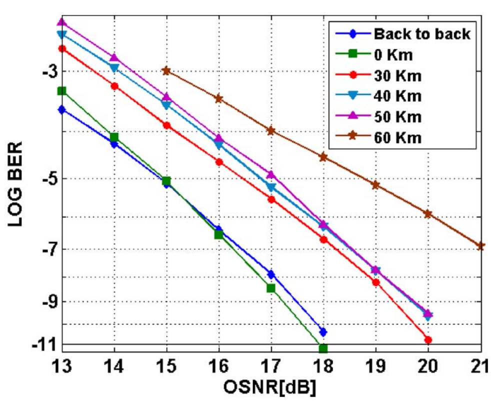

Fig. 6. (Color online) Receiver sensitivity curves for different amounts of fiber CD in the link, compensated by the TODC.

The authors thank Moshe Tur from Tel Aviv University for using their LUNA OVA to carry out GD, PDL, and PMD measurements, and the Israel Science Foundation (ISF) (Grant 1359/07) and the Peter Brojde Center for Innovative Engineering for funding this work.

References

1. C. K. Madsen, G. Lenz, A. J. Bruce, M. A. Cappuzzo, L. T. Gomez, and R. E. Scotti, IEEE Photon. Technol. Lett. **11**, 1623 (1999).
2. K.-M. Feng, J.-X. Chai, V. Grubsky, D. S. Starodubov, M. I. Hayee, S. Lee, X. Jiang, A. E. Willner, and J. Feinberg, IEEE Photon. Technol. Lett. **11**, 373 (1999).
3. K. Takiguchi, K. Jinguji, K. Okamoto, and Y. Ohmori, IEEE J. Sel. Top. Quantum Electron. **2**, 270 (1996).
4. D. J. Moss, S. McLaughlin, G. Randall, M. Lamont, M. Ardekani, P. Colbourne, S. Kiran, and C. A. Hulse, in *Optical Fiber Communications Conference*, A. Sawchuk, ed., Vol. 70 of OSA Trends in Optics and Photonics (Optical Society of America, 2002), paper TuT2.
5. M. Shirasaki, IEEE Photon. Technol. Lett. **9**, 1598 (1997).
6. C. R. Doerr, L. W. Stulz, S. Chandrasekhar, and R. Pafchek, IEEE Photon. Technol. Lett. **15**, 1258 (2003).
7. M. Shirasaki and S. Cao, in *Optical Fiber Communications Conference*, 2001 OSA Technical Digest Series (Optical Society of America, 2001), paper TuS1.
8. D. Marom, C. Doerr, M. Cappuzzo, E. Chen, A. Wong-Foy, L. Gomez, and S. Chandrasekhar, J. Lightwave Technol. **24**, 237 (2006).
9. M. Durst, D. Kobat, and C. Xu, Opt. Lett. **34**, 1195 (2009).
10. C. R. Doerr, R. Blum, L. L. Buhl, M. A. Cappuzzo, E. Y. Chen, A. Wong-Foy, L. T. Gomez, and H. Bulthuis, IEEE Photon. Technol. Lett. **18**, 1222 (2006).
11. D. Sinefeld and D. M. Marom, in *Optical Fiber Communications Conference*, OSA Technical Digest (CD) (Optical Society of America, 2009), paper OThB4.
12. D. Sinefeld and D. M. Marom, IEEE Photon. Technol. Lett. **22**, 510 (2010).
13. K. Suzuki, N. Ooba, M. Ishii, K. Seno, T. Shibata, and S. Mino, in *Optical Fiber Communications Conference*, OSA Technical Digest (CD) (Optical Society of America, 2009), paper OThB3.
14. D. Sinefeld, C. R. Doerr, and D. M. Marom, in *Optical Fiber Communications Conference* (Optical Society of America, 2011), paper OWM6.
15. K. Seno, N. Ooba, K. Suzuki, T. Watanabe, K. Watanabe, and S. Mino, IEEE Photon. Technol. Lett. **21**, 1701 (2009).
16. J. W. Goodman, *Introduction to Fourier Optics*, 3rd ed. (Roberts, 2005).
17. D. T. Neilson, R. Ryf, F. Pardo, V. A. Aksyuk, M. E. Simon, D. O. Lopez, D. M. Marom, and S. Chandrasekhar, J. Lightwave Technol. **22**, 101 (2004).
18. T. Ono, Y. Yano, K. Fukuchi, T. Ito, H. Yamazaki, M. Yamaguchi, and K. Emura, J. Lightwave Technol. **16**, 788 (1998).
19. D. Boivin, M. Hanna, and J. R. Barry, IEEE Photon. Technol. Lett. **17**, 1331 (2005).